

1 **Evaluating the xerophilic potential of moulds on selected egg tempera paints on glass and**
2 **wooden supports using fluorescent microscopy**

3

4 Janez Kosel^{a*}, Maša Kavčič^a, Lea Legan^a, Klara Retko^a and Polonca Ropret^{a,b}

5

6

7 ^a Institute for the Protection of Cultural Heritage of Slovenia, Conservation Centre, Research
8 Institute, Ljubljana, Slovenia

9 ^b Museum Conservation Institute, Smithsonian Institution, Suitland, Maryland, USA

10

11 *Corresponding author: janez.kosel@zvkds.si

12

13

14

15

16

17 Length of the manuscript: 10153 words.

18

19

20

21

22

23

24

25

26

27

28

29

30

31

32 **Highlights**

- 33 • 11 fungal isolates from cultural heritage institutions' interiors were screened for xerophilic trait
- 34 • Specially designed incubators were constructed to hold specific RH levels of 55 %, 63 % and
35 74 %
- 36 • Fungal growth was monitored at low relative humidity on wood and glass supports painted by
37 traditional artists' paints
- 38 • Effects of pigments, support materials and strain variability are discussed

39

40

41

42

43 **Abstract**

44

45 Even though contamination of painted artwork by xerophilic moulds frequently causes aesthetical,
46 physical and/or biochemical biodeterioration, mould growth on paints, prepared from assorted
47 traditional artists' pigments, has yet to be systematically evaluated especially with regard to low
48 relative humidity (RH) levels and painted support materials. Therefore, we investigated 11 fungal
49 strains isolated mostly from cultural heritage institutions' interiors for their potential to grow on
50 egg tempera paint films prepared with different colouring agents and applied on wooden and glass
51 supports which were maintained in monoculture in specially designed incubators at three different
52 RH levels of 55 %, 63 % and 74 %. The growth rate of mould over the surface was assessed using
53 fluorescent microscopy after Calcofluor White staining. Additionally, these stains were screened
54 for their xerophilic and hydrolytic potential using standard microbiological assays. Results show
55 that when comparing growth rates on egg tempera paint films, 6 isolates grew exclusively on wood,
56 exemplifying the greater susceptibility of this supporting material to mould attack. Prussian blue
57 paint also stimulated the growth of 6 isolates, and the maximum overall expansion (38 %) was
58 observed on Prussian blue painted wood. RH was the key factor limiting growth, and at RH of 55
59 % only a slight growth of 2 isolates was observed on Prussian blue painted wood. On the same
60 samples incubated at RH of 63 %, 10 isolates exhibited a moderate to strong growth and 4 of these
61 showed an additional increase in growth at 74 % RH. Paints consisting of artists' pigments carmine
62 lake or lead white in general completely prevented the development of moulds. Nevertheless,
63 tolerance was species/strain dependant and the growths of isolates *Cladosporium halotolerans*
64 EXF-15333, *Aspergillus niger* EXF-14897 and *Aspergillus creber* EXF-15148 on lead white paint
65 (containing ions and salts of heavy metal lead (Pb^{+2})) even exceeds 11 %. Standard microbiological
66 tests showed that all stains had hydrolytic potential and proved positive for xerophilic trait,

67 nevertheless their ability to develop on egg tempera paint films was mostly dependant of very
68 specific conditions.

69

70

71 **Keywords:** Cultural heritage, egg tempera paints, artists' pigments, fluorescent microscopy,
72 xerophiles, fungal overgrowth

73

74

75

76

77

78

79

80

81

82

83

84

85

86

87

88

89

90

91

92

93

94

95

96

97

98

99

100

101

102

103

104

1. Introduction

In museums, fungi can grow and thrive on a wide range of art objects [1–3] and their dispersion is effected by the regular movement of employees and by the ventilation system. Moreover, temperature, RH, and/or light intensity, greatly impact the development of fungi [4–7]. Objects of art, such as oil paintings, works on parchment, painted wood etc., are composed of an array of different organic materials, such as binders, supporting cellulose or collagen based material, glues, pigments and varnishes which represent a rich media prone to fungal colonization [8]. Fungal species can cause aesthetical (stains), physical (hyphal penetration and cracking) and/or biochemical biodeterioration (enzymes and organic acids) [9,10]. Moreover, they are constantly present in the indoor air [11–13], and are considered a potential agent responsible for sick building syndrome, respiratory problems, allergies and certain opportunistic infections at higher spore counts [14–17].

Existing directives on art repository standards are not adequate, because the guidelines do not consider the relevance of micro-niches and the fact that most occurring fungi are microbial extremophiles [6,18]. The majority of fungi need a high RH to develop (water activity $a_w \approx 1$), however extremophiles are able to survive at low water activities and these are classified as xerophilic fungi [19,20]. In fact, some xerophilic species (mainly *Aspergillus* and *Penicillium* spp.) are considered to be primary colonizers since they are capable of growing at $a_w < 0.8$ (RH below 80 %), while some are secondary colonizers (a_w 0.8 - 0.9) [21,22]. Primary colonizers produce metabolic water and thereby increase water activity of the substrate, converting it to a more favourable medium which is suitable for the development of a stable biofilm [23].

129 Conditions on painted cultural heritage items stored in museums comprise of temperatures of
130 around 25 °C and of RH lower than 60 % [24]. In art depots and archives however (usually located
131 below ground level), stored items are subjected to a lower temperature range (around 22 °C) and
132 to a greater fluctuation in RH (can rise above 60%), especially during the summer periods for
133 which HVAC (Heating, ventilation, and air conditioning) system failures are more common and
134 can last up to 2 weeks. Frequent failures include leaking refrigerant, clogged air filter, frozen coils
135 and faulty motor capacitors [25]. Therefore, in such conditions (RH between 55 % and 70 %), the
136 xerophilic potential of a fungal species is an important advantage, enabling its establishment on
137 valuable art objects. Nevertheless, for fungal isolates emerging from cultural heritage institutions,
138 this trait has never been addressed properly, and most studies have only focused on strains isolated
139 from mural paintings [26–31], their molecular identification, defining their enzymatic activities
140 for protein (test for gelatin hydrolysis) [32–39] and cellulose biodegradation [36,40–43], as well
141 as traits which define their pathogenicity to human health (growth at 37°C, phospholipase and
142 hemolytic activities) [44,45]. The xerophilic potential has only been described by standard assays,
143 which employ simple selective solid media with high concentrations of sodium chloride or
144 glucose, which lower the a_w of a medium at an optimum temperature range for mould growth (28
145 °C) [46]. Additionally, to our knowledge, no study has systematically investigated the influence of
146 different artists' paints and their individual components (e.g. various pigments) on mould growth,
147 especially in relation to low RH levels and different painting supports.

148

149

150

151

152 **2. Research aim**

153
154
155 The aim of this study was to see if fungal species, with standardly proven xerophilic trait (standard
156 microbiological assay on high osmolarity media with reduced water activity), can develop and
157 grow on selected materials comprising painted cultural heritage items in conditions which prevail
158 in museums or in art depos (temperature of around 23 °C and RH levels between 50 % and 70 %).
159 With this aim, we devised special incubators with saturated salt solutions, which can hold painted
160 model samples at specific RH levels. Different support (inert glass or hygroscopic wood) and paint
161 (whole egg tempera paints employing 3 historically popular artists' pigments) materials were
162 tested for their impact on mould growth. Finally, the ability of these fungal species to utilise
163 nutrients contained within the whole egg tempera paint film was assessed using standard
164 microbiological Petri plate assays (for proteolytic and lipolytic activities).

165
166
167
168
169
170
171
172
173
174
175
176
177
178
179
180
181
182
183
184
185
186
187

188 **3. Material and methods**

189
 190
 191 **3.1 Fungal isolates**
 192
 193 Strains isolated from the following artefacts and environments were used to inoculate the surfaces
 194 of prepared model samples: the Celje ceiling (Slovenia), air in the depot of the restoration centre,
 195 oil paintings on canvas, a 17th century parchment, a wooden African sculpture, Sečovlje salterns
 196 (Gulf of Trieste), fruits and nursing cream (see Table 1 for details). Isolates designated as ZIM
 197 were supplied from the Collection of Industrial-Microorganisms-Slovenia and isolates designated
 198 as EXF were supplied from the Infrastructural Centre Mycosmo-Culture-Collection, Slovenia. All
 199 were grown to sporulation on malt extract agar (MEA, 30 g/L of malt extract (Sigma Aldrich) and
 200 15 g/L of agar (Sigma Aldrich)) solid medium at 26 °C.

201

202

203 Table 1: Eleven fungal strains isolated mostly from cultural heritage institutions' interiors.

Isolate designation	Identified species	Source	Isolation procedures	Identification method	Collected by/ Reference
EXF-10689	<i>Engyodontium album</i>	The Celje Ceiling in the main chamber of the Old Counts' Mansion, CRM	Dilution plates (MEA) after swabbing as described by Jurjević et al. [47], and DNA isolation from colonies	ITS (primers ITS1, NL4 and ITS4) amplification and sequencing described in Sklenář et al. [48]	P. Zalar ^A , M. Matul ^A (May 2014)
EXF-15047	<i>Aureobasidium melanogenum</i>	Air in the depot of the RC of IPCHS	Bio-aerosol impaction sampler as described by Peterson & Jurjević [49], plating on MEA and DNA isolation from colonies	ITS (primers ITS1, NL4 and ITS4) amplification and sequencing described in Sklenář et al. [48]	P. Zalar ^A , M. Matul ^A (May 2014)
ZIM-F94	<i>Penicillium crustosum</i>	Fruits from the DFST, BFL	Dilution plates (MEA) of homogenized matter and DNA isolation from colonies	18S-ITS1-5.8S-ITS2 rDNA (primers NS1 and ITS4) amplification and endonuclease restriction analysis described in Raspor et al. [50]	N. Čadež ^B
EXF-7651	<i>Aspergillus destruens</i>	Oil painting on canvas of the NGS	Dilution plates (MEA) after swabbing as described by Jurjević et al. [47], and DNA isolation from colonies	ITS (primers ITS1, NL4 and ITS4) and benA (primers Bt2a, T10 and Bt2b) amplification and sequencing described in Sklenář et al. [48]	[48]
EXF-10623	<i>Aspergillus halophilicus</i>	17th century nobel diploma written on parchment from the ARS	Dilution plates (MEA) after swabbing as described by Jurjević et al. [47], and DNA isolation from colonies	ITS (primers ITS1, NL4 and ITS4) and benA (primers Bt2a, T10 and Bt2b) amplification and sequencing	P. Zalar ^A , M. Matul ^A (May 2014)

				described in Sklenář et al. [48]	
EXF-10201	<i>Wallemia</i> sp.	Oil painting on canvas from the RC of IPCHS	Dilution plates (MEA) after swabbing as described by Jurjević et al. [47], and DNA isolation from colonies	ITS (primers ITS1, NL4 and ITS4) amplification and sequencing described in Sklenář et al. [48]	P. Zalar ^A , M. Matul ^A (May 2014)
EXF-150	<i>Aureobasidium pullulans</i>	Sečovlje salterns (Gulf of Trieste)	Dilution plates (MEA) and DNA isolation from colonies	ITS (primers ITS1, NL4 and ITS4) amplification and sequencing described in Sklenář et al. [48]	[51]
EXF-14897	<i>Aspergillus niger</i>	Sečovlje salterns (Gulf of Trieste)	Dilution plates (MEA) and DNA isolation from colonies	ITS (primers ITS1, NL4 and ITS4) and benA (primers Bt2a, T10 and Bt2b) amplification and sequencing described in Sklenář et al. [48]	P. Zalar ^A , M. Matul ^A (May 2014)
EXF-15333	<i>Cladosporium halotolerans</i>	Oil painting on canvas (Vittore Carpaccio) from the RC of IPCHS	Dilution plates (MEA) after swabbing as described by Jurjević et al. [47], and DNA isolation from colonies	ITS (primers ITS1, NL4 and ITS4) and Act (primers ACT-512F and ACT-783R) amplification and sequencing described in Sklenář et al. [48]	P. Zalar ^A , M. Matul ^A (May 2014)
EXF-15148	<i>Aspergillus creber</i>	Religious wooden sculpture from Mali, (first half of the 20th cent., SEM)	Dilution plates (MEA) after swabbing as described by Jurjević et al. [47], and DNA isolation from colonies	ITS (primers ITS1, NL4 and ITS4) and benA (primers Bt2a, T10 and Bt2b) amplification and sequencing described in Sklenář et al. [48]	P. Zalar ^A , M. Matul ^A (May 2014)
ZIM-F42 = [52]	<i>Aspergillus niger</i>	Nursing cream from the DFST, BFL	Dilution plates (MEA) of homogenized matter and DNA isolation from colonies	18S-ITS1-5.8S-ITS2 rDNA (primers NS1 and ITS4) amplification and endonuclease restriction analysis described in Raspor et al. [50]	N. Čadež ^B

204

205 Abbreviations: National Gallery of Slovenia (NGS); Restoration Centre (RC) of the Institute for the protection of Cultural Heritage of Slovenia
 206 (IPCHS); Archives of the Republic of Slovenia (ARS); The Department of Food Science and Technology (DFST); Biotechnical Faculty of Ljubljana
 207 (BFL); Slovene Ethnographic Museum (SEM); Internal transcribed spacer (ITS); β -tubulin (benA); Actin (Act); Fungal ribosomal operon (18S-
 208 ITS1-5.8S-ITS2); Chloramphenicol and dichloran-glycerol agar medium (DG18); Collection of Industrial-Microorganisms-Slovenia (ZIM,
 209 <https://www.zim-collection.si/>); and Infrastructural Centre Mycosmo-Culture-Collection, Slovenia (EXF, <https://www.ex-genebank.com/>).

210 ^AMicrobiology, Department of Biology; Chair of Molecular Genetics and Microbiology, Večna pot 111, Ljubljana, Slovenia; ^BDFST, Chair of
 211 Biotechnology, Microbiology and Food Safety, Jamnikarjeva 101, Ljubljana, Slovenia.

212

213

214 3.2 Determination of the xerophilic and hydrolytic potential

215

216 The xerophilic trait was determined using two petri dish assays, one containing saturated salts
 217 (NaCl) and the other one containing saturated sugars. For the first test, 10 μ L of spore
 218 inoculation suspension was carefully pipetted onto a sterile Potato Dextrose Agar plate (PDA;
 219 200 g/L of potato infusion, 20 g/L of dextrose and 15 g/L of agar) supplemented with 12 % NaCl
 220 (120 g/L) [53]. For the second test, the same was performed, however, a sterile high sugar

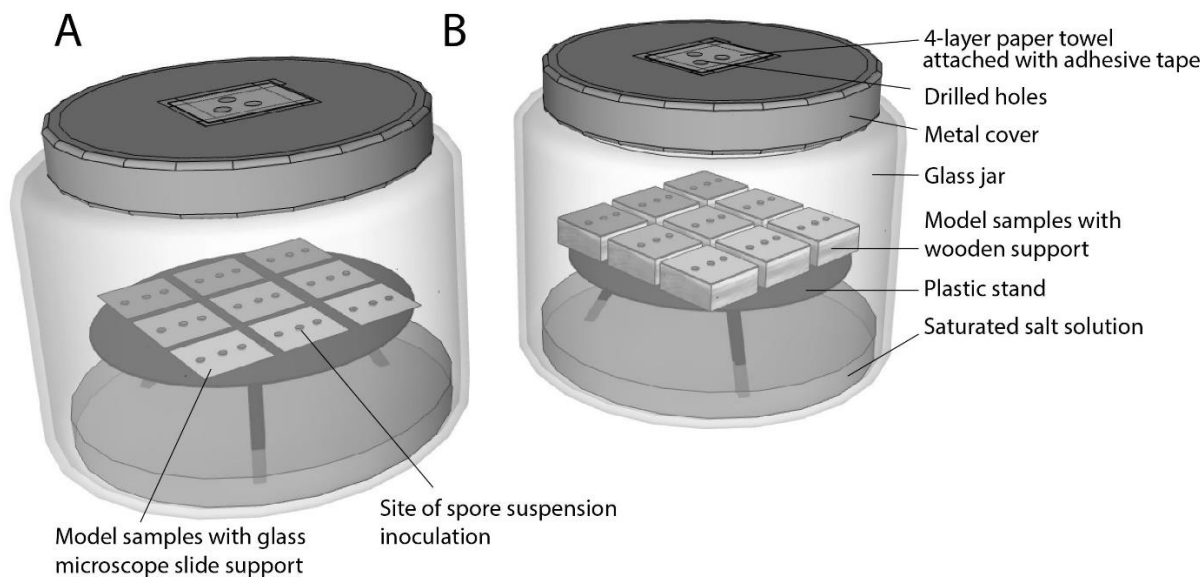
221 osmolarity CY20S medium containing 1 g/L of K_2HP0_4 , 3 g/L of $NaNO_3$, 0.5 g/L of
222 $MgSO_4 \cdot 7H_2O$, 0.5 g/L of KCl, 0.01 g/L of $FeSO_4 \cdot 7H_2O$, 5 g/L of yeast extract, 15.0 g/L of agar
223 and 200 g/L of sucrose was used instead [53]. Petri plates from both tests were then incubated for
224 14 days at 28 °C, and after incubation the fungal growth was assessed. For the gelatin hydrolysis
225 test (standard test for proteolytic activity), agar plates were prepared by mixing autoclaved
226 Reasoner's 2A agar (R2A; contains 0.05 % of proteose peptone, 0.05 % of casamino acids, 0.05
227 % of yeast extract, 0.05 % of dextrose, 0.05 % of soluble starch, 0.03 % of dipotassium
228 phosphate, 0.005 % of magnesium sulfate, 0.03 % of sodium pyruvate and 1.5 % of agar, Sigma
229 Aldrich) with 0.4 % of sterilized gelatin (Sigma Aldrich). After a 10 μ L spore inoculation and a
230 14 days long incubation at 28 °C, the hydrolysis zone was visualized by using a 10% tannin
231 solution, which was flooded onto the agar plates [54]. For lipolytic activity testing, Spirit Blue
232 agar was prepared by suspending 32.15 g of Spirit Blue agar (Spirit Blue being the indicator of
233 lipolysis) (Sigma-Aldrich) in 1000 mL distilled water, autoclaved, cooled down to 50 °C and
234 supplemented with 30 ml of lipase substrate (1 mL of Tween 80, 400 mL of warm distilled water
235 and 100 mL of olive oil; sterilized by autoclaving). This was slowly mixed and poured into Petri
236 dishes [54]. After a 10 μ L spore inoculation and a 14 days long incubation at 28 °C, the halos
237 around the grown mycelia indicated lipolysis.

238 239 **3.3 Construction and testing of incubators**

240
241
242 In figure 1, an air-permeable (perforated) incubator is presented, which is basically a 370 ml
243 household glass jar (cat. no. 3029550 Merkur, Slovenia) with 3 holes (2 mm in diameter) drilled
244 in the middle of its metal cover. The holes were covered on top with a 4-layer laboratory paper
245 towel which was attached onto the cover with an adhesive tape. This perforation was necessary for

246 the growth of fungi, as it allows the exchange of respiratory gases. The bottom of the jar was filled
 247 with 20 ml of the appropriate saturated salt solution for maintaining specific RH, and a plastic
 248 stand was inserted (Avacom cat. no. 561934 Merkur, Slovenia). A saturated solution of NaCl, KI
 249 or K₂CO₃ was used. For KI (Sigma Aldrich, 207969) 190.5 g of salt was added to 100 ml of MilliQ
 250 water; for NaCl (Sigma Aldrich, 7760) 50 g of salt was added to 100 ml of MilliQ water; and for
 251 K₂CO₃ (Sigma Aldrich, 209619) 155.5 g of salt was added to 100 ml of Milli-Q water. For each
 252 solution, RH within the enclosed (cover attached) incubator was measured by using a household
 253 RH meter (Techno Line, Spar Slovenia) which was placed on top of the plastic stand. The
 254 measurement was taken after a two day long incubation at 23 °C.

255
 256
 257
 258
 259



260
 261
 262
 263
 264
 265
 266
 267

Figure 1: Incubator with paint samples on glass (A) and wood (B).

268 **3.4 Preparation of model samples**

269
270
271 Two series of model samples were prepared, the first represented paints applied on glass supports
272 (non-hygroscopic material), the second the same paints on wooden supports (hygroscopic
273 material). Glass supports were made from objective glass slides (Art No. 42401010;
274 Glasswarefabrik Karl Hecht GmbH & Co KG) that were cut down into sizes of 25 x 25 x 1 mm
275 and cleaned with distilled water and 96% (v/v) ethanol (ACS Reagent) subsequently. Wooden
276 supports were prepared from naturally aged untreated (no coatings present) spruce boards, which
277 were cut to rectangular blocks of approximate dimension 25 x 25 x 13 mm. The blocks were then
278 sanded with sand paper and cleaned with compressed air to remove any of the remaining dust
279 particles.

280
281 For the preparation of paints, we chose plain whole egg as a tempera binder without any other
282 possible additives (no water and no preservatives). Although traditional tempera painting has
283 always been associated mainly with egg yolk, recipes, comprehensively recorded since the
284 Middle Ages in the treatises such as by Cennino Cennini, Giorio Vasari and Giovanni Armenini
285 among others, and hitherto put into practice in many variations, frequently involve the use of
286 whole egg as the sole or the main binder of the tempera paints as well [55]. The reason to employ
287 whole egg as the binder was also microbiological. Whole egg is a rich source of both proteins
288 (egg white) and fat (egg yolk), and therefore, by choosing whole egg, we allowed for the
289 development of both proteolytic and lipolytic fungal isolates on the painted surfaces. Binder
290 preparation was as follows: 2 free-range chicken eggs were separated from the shell and then
291 thoroughly mixed using a household mixer. After the setting of the liquid, the obtained binder
292 was further mixed with each of the three selected pigments into three paints using a metal spatula

293 and grinded with a glass muller on a glass plate to an adequate paint consistency (all tools were
294 cleaned with tap water and detergent, and washed with distilled water). The binder to pigment
295 weight ratio in the paint was $\approx 1 : 0.8$. The following pigments were used: for paint containing
296 lead white type of pigment (basic lead carbonate, $(\text{PbCO}_3)_2 \cdot \text{Pb}(\text{OH})_2$; PW1, C.I. 77597)
297 Cremnitz White (Kremer Pigmente GmbH & Co.KG; Art.No. 46000.13010.120), for paint
298 containing pigment Prussian blue (iron (III) hexacyanoferrate (II), $\text{Fe}_4[\text{Fe}(\text{CN})_6]_3$; PB27, C.I.
299 77510) Prussian blue LUX (Kremer Pigmente GmbH & Co.KG; Art.No. 45202.12100.136) and
300 for paint containing carmine lake type of pigment (red lake (aluminium lake) of carminic acid
301 (carmine lake) of cochineal origin; NR4, C.I. 75470) Carmine Naccarat (Kremer Pigmente
302 GmbH & Co.KG; Art.No. 42100.12100.136). Lead white was chosen as the principal European
303 colouring agent of white colour from antiquity until modern times. We selected Prussian blue as
304 a leading representative of traditional blue pigments in European painting since its discovery in
305 the beginning of the 18th Century, while carmine lakes (with the exception of vermilion) were
306 probably the most used red artists' pigments between the 16th Century and the discovery of
307 synthetic alizarin in the 19th Century. The colouring agents were also selected according to
308 colour, chemical composition and possibility to be more or less susceptible to mould growth
309 (dark/light colour, involving heavy metals, organic/inorganic constituents, iron ions etc.).
310 Prepared paints were applied with brush (Utrecht Manglon 2630-B No. 10) directly on the
311 frontal planes of glass or wooden supports in a single layer application. To better evaluate the
312 effects of pigments within paints, control samples with egg binder alone were prepared as well,
313 applied to glass and wooden supports without the presence of the pigments. All of the prepared
314 samples were left to dry at room temperature on covered plastic stands for a period of 2 weeks.
315 After drying, one series of 10 glass and one series of 10 wooden samples (3 repetitions of model

316 samples for each of the three paint varieties: lead white, Prussian blue and carmine lake; plus one
317 control sample) were each placed within the prepared incubators with saturated salt solutions.
318 The enclosed incubators were sterilised in autoclave (121 °C, 1.1 bar, 15 min).

319

320 **3.5 Inoculation of model samples**

321 Spores of fungal monocultures on MEA plates were collected and were stored at 4 °C in skimmed
322 milk (1 mL) which was instantly dehydrated by mixing it with 10 mL of anhydrous granular silica
323 gel. Prior to mixing, the latter was dry-heat sterilised at 175 °C for 2 h in 15 mL glass vials [56],
324 turning it into yellow granules. To prepare for the inoculation, 0.5 mL of granules containing
325 spores were suspended in 0.5 ml of Milli-Q water, spore count was determined under the
326 microscope Zeiss LSM 800 using a standard Bürker-Türk counting chamber (hemocytometer) [57]
327 and the final spore concentration was adjusted to around 1×10^7 spores/mL by additional dilutions
328 in Milli-Q water.

329

330 For the final inoculation, sterile incubator was opened in aseptic conditions and 10 µL of spore
331 inoculation suspension (monoculture) was carefully pipetted onto each painted surface (three
332 inoculation spots for each model sample; see Figure 1). The incubator was then sealed with the lid
333 and placed in the dark at 23 °C. Each incubator contained model samples which were inoculated
334 with only one fungal monoculture (isolate). The entire inoculation period of the samples spanned
335 over 120 days.

336

337 **3.6 Sampling from incubators**

338

339 Examination of mould growth rate on model samples was performed three times for each incubator
340 and through the entire incubation time (120 days). First sampling took place after 28 days, second

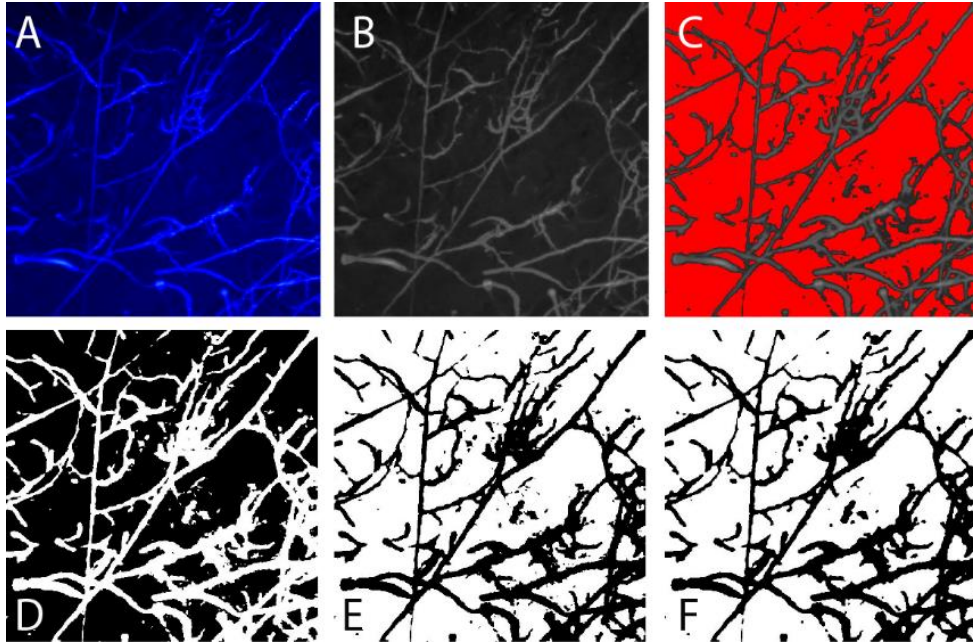
341 after 68 days, and third after 120 days of incubation. When sampling, the incubator was opened in
342 aseptic conditions and 1 model sample was removed from the incubated series. Immediately after,
343 the incubator was resealed and placed back in the dark at 23 °C. The removed sample was further
344 analysed under the fluorescent microscope to determine the percentage of mould expansion over
345 the painted surface.

346
347
348
349
350

3.7 Analysis of mould growth using fluorescent microscopy

351 The exact percentage of inoculated mould formation on the surface of the model samples was
352 determined using the fluorescent microscope analysis, for which the sample was firstly stained
353 using a fluorescent dye Calcofluor White, which specifically binds to the chitin cell wall of the
354 mould (Figure 2). For this purpose, 10 µL of Calcofluor White dye, previously mixed in a 1:1
355 ratio with 10% KOH, was pipetted onto the surface of a model sample at the inoculation spots.
356 Staining was analysed using the Zeiss LSM 800 confocal fluorescence microscope with a
357 fluorescence filter with an emission maximum of 460 nm and a 50x magnification. The
358 individual images for each slide were analysed with an open source image processing package
359 of ImageJ called Fiji (version 1.52c) [58], to obtain the mould surface coverage using a triangle
360 method and an ImageJ measuring function [59]. The images were converted to binary format
361 with a black background and white biofilm, with an automatically determined threshold value
362 that separates the biofilm from the background. Visual noise was removed from all the images in
363 the set, using the “despeckle” function. Considering the entire field of view of the image, we
364 then calculated the mould surface coverage percentage using the "measure" function, and from 3
365 images the average percentage of coverage was calculated.

366



367
368
369
370
371
372
373
374
375
376
377
378
379
380
381
382
383

Figure 2: Fluorescent microscopic photographs used for determination of percentage of mould surface coverage (on the photographs, *A. destruens* after 68 days of incubation on wood painted with Prussian blue at an RH level of 63 % is presented). A: original photograph; B: black and white 8 bit photograph; C: boundary focus determination between the mould and the background; D: binary format with black background and white mould; E: inverted image; and F: noise removal.

384 4. **Results**

385
386 Initially, within each incubator containing a saturated solution of either NaCl, KI or K₂CO₃, RH
387 was measured after a two day long incubation at 23 °C. The established humidity levels within the
388 enclosed incubators (measured using the Rh meter) were 55 %, 63 % and 74 % for K₂CO₃, KI and
389 NaCl, respectively.

390
391 Standard screening of the 11 fungal isolates for xerophilic and hydrolytic potential revealed that
392 all isolates could tolerate NaCl or sucrose induced osmolarity and demonstrated at least one
393 biodegradative property (Table 1). Most of the isolates, with the exception of *A. halophilicus*
394 EXF-10623, could easily grow in 12 % NaCl. However, when the medium was supplemented
395 with 20 % of sucrose, the growth of 6 isolates was severely delayed. Isolates with the most active
396 proteolytic activity were *E. album* EXF-10689, *C. halotolerans* EXF-15333, *P. crustosum* ZIM-
397 F94 and *A. niger* ZIM-F42; and isolates exhibiting the highest lipolytic activity were *Wallemia*
398 sp. EXF-10201, *Aureobasidium melanogenum* EXF-15047, *Aspergillus niger* ZIM-F42 and *E.*
399 *album* EXF-10689. Interestingly, no proteolytic reaction was observed for *Wallemia* sp. EXF-
400 10201.

401

402

403

404

405

406

407

408 Table 2: Xerophilic and hydrolytic potential of examined fungal isolates.
 409

Isolates	NaCl induced osmolarity	Sucrose induced osmolarity	Proteolytic activity	Lipolytic activity
<i>Engyodontium album</i> EXF-10689	+++	+	++	++
<i>Aureobasidium melanogenum</i> EXF-15047	+++	++	+	++
<i>Penicillium crustosum</i> ZIM-F94	+++	+++	++	+
<i>Aspergillus destruens</i> EXF-7651	+++	++	+	+
<i>Aspergillus halophilicus</i> EXF-10623	+	+++	+	+
<i>Wallemia</i> sp. EXF-10201	+++	+	-	+++
<i>Aureobasidium pullulans</i> EXF-150	+++	+	+	+
<i>Aspergillus niger</i> EXF-14897	+++	+	+	+
<i>Cladosporium halotolerans</i> EXF-15333	+++	+	++	+
<i>Aspergillus creber</i> EXF-15148	+++	+	+	+
<i>Aspergillus niger</i> ZIM-F42	+++	++	++	++

410
 411 Legend: +++: quick and extensive positive reaction for hydrolytic activities (for osmolarity:
 412 extensive growth and sporulation); ++: strong positive reaction (for osmolarity: obvious growth);
 413 +: weak positive reaction (for osmolarity: observable micelium); -: no reaction (for osmolarity:
 414 no growth).

415
 416 The effect of a specific RH, established within the incubator, on inoculated mould growth kinetics
 417 is presented in figure 3. Mould growth is represented in the form of mould expansion percentage,
 418 covering the surface of painted model samples and calculated from images obtained under
 419 fluorescent microscopy.

420
 421 For wood painted with Prussian blue, at RHs of 63 % and 74 %, a steady growth of *E. album* EXF-
 422 10689 (Figure 3, Graph A), *Aureobasidium melanogenum* EXF-15047 (Figure 3, Graph B) and

423 *Aspergillus halophilicus* EXF-10623 (Figure 3, Graph E) reaching between 5-10 % was observed
424 (after 120 days of incubation). For the same model samples and RH conditions, the growth of *P.*
425 *crustosum* ZIM-F94 (Figure 3, Graph C) and *A. destruens* EXF-7651 (Figure 3, Graph D) after 68
426 days of incubation reached around 20 % of surface coverage and the growth of *Wallemia* sp. EXF-
427 10201 exceeded 35 % (Figure 3, Graph F). On all other model samples (lead white and carmine
428 lake on wood and glass supports), regardless of the employed humidity, strains *E. album* EXF-
429 10689, *A. melanogenum* EXF-15047 and *P. crustosum* ZIM-F94 exhibited no surface growth. At
430 RHs of 63 % and 74 %, *Aspergillus destruens* EXF-7651 (Figure 4) and *Aspergillus halophilicus*
431 EXF-10623 steadily grew to 5-10 % surface coverage on wood painted with carmine lake.
432 Regardless of the supporting material used, at RH of 74 %, *A. pullulans* EXF-150 grew well
433 (around 20 % expansion) on Prussian blue paint, and also grew slightly (around 5 % growth) on
434 lead white paint (Figure 3, Graph G). However, at RH of 63 % growth was only detected on wood
435 covered by Prussian blue tempera. Similar results were obtained for the formation of *A. niger* EXF-
436 14897 (Figure 3, Graph H). The main differences in comparison to the growth of *A. pullulans*
437 EXF-150 were that *A. niger* EXF-14897 reached an overall lower surface coverage (11 %) on
438 wood-Prussian blue samples at RH of 74 %, and that its growth was non-existent on glass-Prussian
439 blue samples at the same RH.

440 Interestingly, even at RH of 63 %, *C. halotolerans* EXF-15333 exhibited a moderate (10 %
441 coverage on glass) to strong (20 % coverage on wood) surface growth on lead white paint (Figure
442 3, Graph I). As with most isolates, *C. halotolerans* EXF-15333 only grew if Prussian blue was
443 applied to wood (RHs of 63 % and 74 %).

444 *Aspergillus creber* EXF-15148 grew strongly on every single model sample exposed to RHs of 63
445 % or 74 %. Furthermore, on all model samples containing wood (at 74 % RH) its growth exceeded

446 33 % of surface coverage (Figure 3, Graph J). In contrast to *A. creber* EXF-15148, *A. niger* ZIM-
447 F42 exhibited no surface growth and even at RH of 74 %, the conditions were still too dry for its
448 development (Figure 3, Graph K).

449 When RH was as low as 55 %, only isolates *Wallemia* sp. EXF-10201 and *A. creber* EXF-15148
450 exhibited a slight development of around 1 % surface coverage (exclusively on wood-Prussian
451 blue samples).

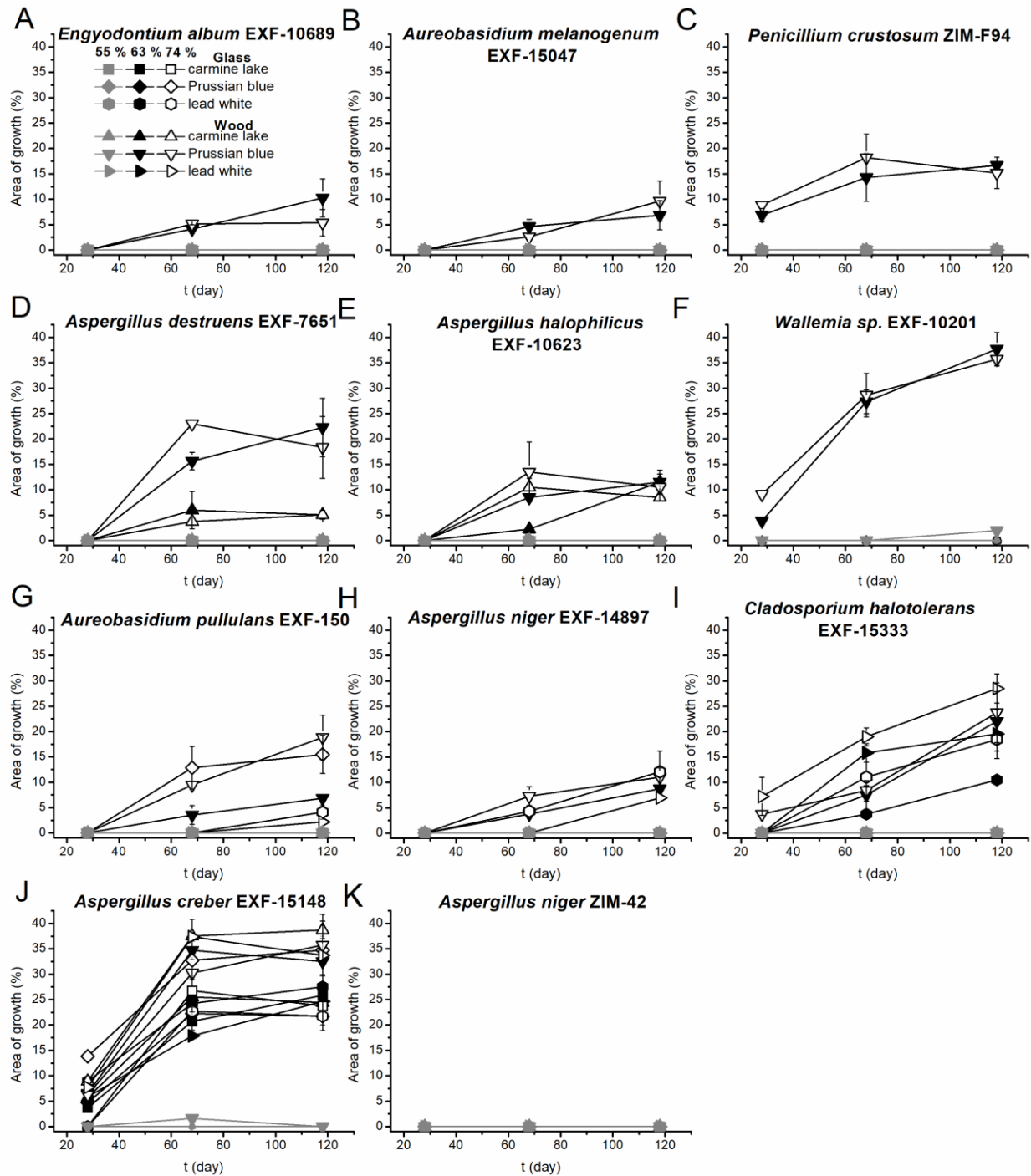
452

453

454

455

456

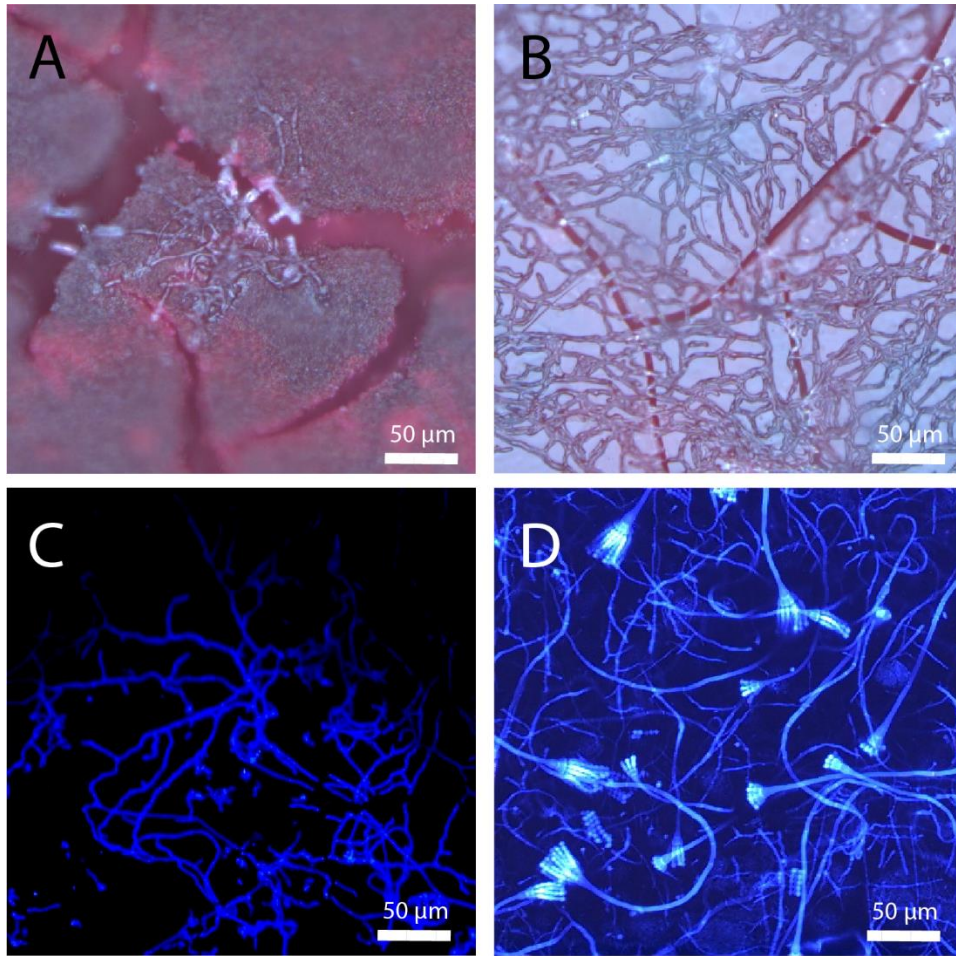


457

458 Figure 3: Percentage of growth of 11 fungal isolates on wooden and glass model samples painted
 459 with egg temperas containing three different pigments (lead white, Prussian blue, carmine lake).

460 Incubation continued for 120 days at a specific RH (55 %, 63 % or 74 %) and percentage of fungal

461 expansion over the surface was determined under the fluorescent microscope.



462

463 Figure 4: Fungal growth on wood based model samples under optical and fluorescent microscopy.

464 Initial (A; 28 days on incubation) and developed (B; 68 days on incubation) growth of *A. destruens*

465 EXF-7651 on wood with carmine lake egg tempera at RH of 74 % and analysed under optical

466 microscopy. Overgrowth of EXF-7651 (C) and *P. crustosum* ZIM-F94 (D) (68 days on incubation

467 at RH of 74 %; carmine lake egg tempera on wood) under fluorescence microscopy after

468 Calcofluor White staining.

469

470 To evaluate how pigments within paint films effect mould growth, 11 fungal isolates were also

471 inoculated onto glass and wood control samples containing only a layer of the egg binder (egg

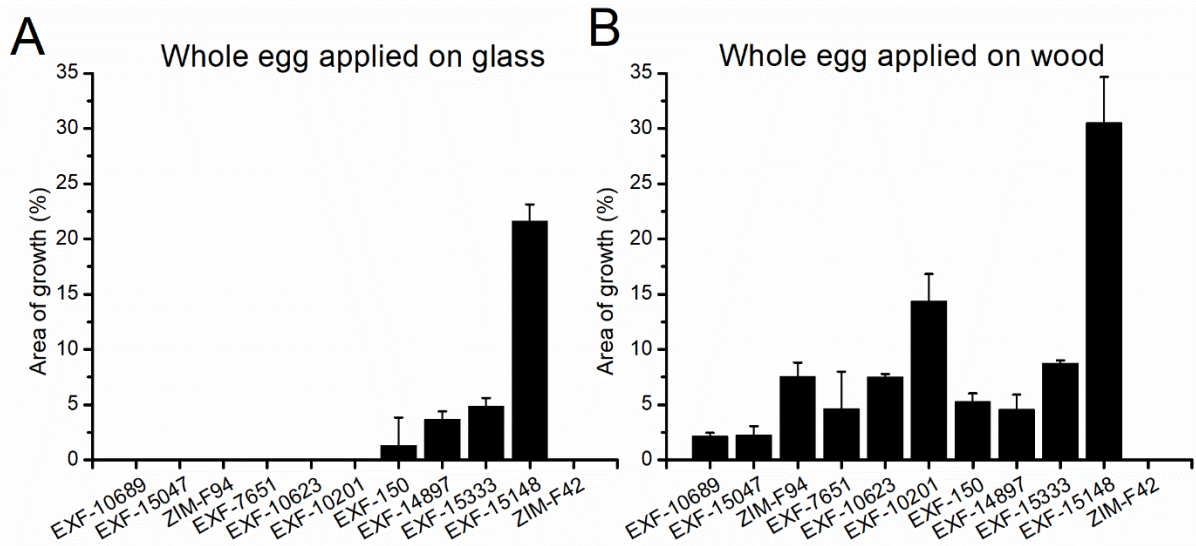
472 white and egg yolk mixture). These control samples were then incubated at an RH of 74 % for 68

473 days (at 23 °C) and the percentage of fungal surface overgrowth was measured using the
474 fluorescent microscope (Figure 5). RH of 74 % was chosen for incubation because we initially
475 thought that at lower RH levels (55 % and 63 %) surface mould growth would be minimal or non-
476 existent, and therefore the inhibiting effects of pigments on mould growth would be difficult to
477 measure.

478

479 On glass based control samples, isolates *Aureobasidium pullulans* EXF-150 (1.3 %), *Aspergillus*
480 *niger* EXF-14897 (3.6 %), and *C. halotolerans* EXF-15333 (4.8 %) exhibited a slight surface
481 growth and isolate EXF-15148 showed a moderate rate of growth (21.5 %) (Figure 5, Graph A).
482 However, when wood control samples were used for incubation, all isolates, with the exception of
483 *A. niger* ZIM-F42, were able to exhibit low (*E. album* EXF-10689, *Aureobasidium melanogenum*
484 EXF-15047, *Aspergillus destruens* EXF-7651, *Aureobasidium pullulans* EXF-150 and *Aspergillus*
485 *niger* EXF-14897) to moderate (*P. crustosum* ZIM-F94, *Aspergillus halophilicus* EXF-10623,
486 *Wallemia* sp. EXF-10201, *C. halotolerans* EXF-15333 and *Aspergillus creber* EXF-15148)
487 surface growth (Figure 5, Graph B).

488



489

490 Figure 5: Percentage of growth of 11 fungal isolates on glass (A) and wooden (B) control samples
 491 containing only a layer of the whole egg binder. Incubation at RH of 74 % was terminated after 68
 492 days and the percentage of fungal formation on the surface was determined under the fluorescent
 493 microscope.

494

5. Discussion

495
496
497
498
499
500
501
502
503
504
505
506
507
508
509
510
511
512
513
514
515
516
517

Standard screening for xerophilic potential revealed that all of the isolates could easily tolerate and show extensive growth in high osmolarity medium induced by NaCl. For species such as *Aureobasidium pullulans* [60], *A. melanogenum* [61], *E. album* [62], *Aspergillus* spp., *Cladosporium* spp. [63], *P. crustosum* [64], *Wallemia* spp. [65], *Aspergillus niger* [66], and *A. creber* [67] this is a commonly observed trait. When sucrose was used to induce osmolarity, the growth of 6 isolates was delayed and only the growth of *P. crustosum* ZIM-F94 and *A. halophilicus* EXF-10623 was non-restricted. In contradiction to the observations of Smolyanyuk and Bilanenko [68], that *A. halophilicus* is a salt tolerant species, our tests show a clear preference of *A. halophilicus* EXF-10623 to sucrose based osmolarity.

Standard screening for hydrolytic potential revealed that all isolates (with the exception of *Wallemia* sp. EXF-10201 (only lipolytic)) exhibited both proteolytic and lipolytic activities. The most proteolytic isolates proved to be *E. album* EXF-10689, *C. halotolerans* EXF-15333, *P. crustosum* ZIM-F94 and *A. niger* ZIM-F42. The proteolytic activities for these species were also confirmed by Chellappan et al. [69] (for *E. album*), by Borrego et al. [45] (for *A. niger*), by Jaouani et al. [63] (for *C. halotolerans*) and by Park et al. [70] (for *P. crustosum*). Furthermore, we observed a strong lipolytic activity for *Wallemia* spp. EXF-10201, *Aureobasidium melanogenum* EXF-15047, *E. album* EXF-10689 and *Aspergillus niger* ZIM-F42, and similar observations were made by Chamekh et al. [71] (for *Wallemia* spp.), Vitisant et al. [72] (for *Aureobasidium melanogenum*), Alapont et al. [73] (for *E. album*) and by Mahadik et al. [74] (for *Aspergillus niger*).

518 The effect of a specific RH, established within the incubator, on mould growth kinetics on painted
519 model samples, revealed that at RH of 55 % almost no growth was observed and only a slight
520 development was observed for isolates *Wallemia* sp. EXF-10201 and *A. creber* EXF-15148.
521 Nevertheless, it is surprising that for 6 (*E. album* EXF-10689, *Aureobasidium melanogenum* EXF-
522 15047, *P. crustosum* ZIM-F94, *Aspergillus destruens* EXF-7651, *A. halophilicus* EXF-10623 and
523 *Wallemia* sp. EXF-10201) out of 11 isolates fungal formation percentage was similar between RH
524 levels of 63 % and 74 %. This is in contradiction to Strang [75], who made an extensive literature
525 review on mould development in relation to RH, and noticed a clear linear progression in mould
526 growth from 55 % to 100 % RH. Nonetheless, for isolates *Aureobasidium pullulans* EXF-150,
527 *Aspergillus niger* EXF-14897, *A. creber* EXF-15148 and *C. halotolerans* EXF-15333 growth in
528 general was promoted when RH was increased from 63 % to 74 %.

529
530 Regardless of the RH levels tested (even at 55 % RH), our results show that the bioreceptivity (the
531 ability of a material to be colonised by living organisms [76]), of glass or wood support materials
532 within laboratory samples is vastly different. In fact, when comparing glass and wood based
533 control samples, glass did not prove to be bioreceptable for 6 isolates (*E. album* EXF-10689,
534 *Aureobasidium melanogenum* EXF-15047, *P. crustosum* ZIM-F94, *Aspergillus destruens* EXF-
535 7651, *A. halophilicus* EXF-10623 and *Wallemia* sp. EXF-10201) which otherwise exhibited
536 significant growth (colonisation) on wood supports. Higher bioreceptivity of wood in comparison
537 to glass was also observed on model samples containing pigments (Prussian blue: 3.4 % higher
538 growth of *Aureobasidium pullulans* EXF-150; lead white: 10.0 % higher growth of *C. halotolerans*
539 EXF-15333 and *Aspergillus creber* EXF-15148; carmine lake: 10.0 % higher growth of *A. creber*
540 EXF-15148).

541 Wood is a hygroscopic material which changes mass and volume depending on the surrounding
542 RH, meaning it is a material that absorbs water [77]. Water gets into wood in three ways: as a fluid
543 through the cell lumens through capillary tension, as vapour through the cell lumens, and as
544 molecular diffusion through the cell walls. This makes wood a highly bioreceptable material on
545 which mould mediated biodegradation of dried substrates (organic binders) can occur even at low
546 RH levels [78].

547
548 Pigments strongly inhibited or increased the growth of moulds. This was especially evident when
549 incubations on wood based control samples (without pigment) were compared with incubations on
550 wood based model samples (with pigment). For instance, at RH of 74 %, Prussian blue increased
551 the growth of isolates *P. crustosum* ZIM-F94, *Aspergillus destruens* EXF-7651, *A. halophilicus*
552 EXF-10623, *Wallemia* sp. EXF-10201 and *Aureobasidium pullulans* EXF-150 by 10.6 %, 18.3 %,
553 6 %, 14.2 % and by 4.2 %, respectively. In contrast to Prussian blue, however, pigments carmine
554 lake and lead white generally completely prevented the growth of moulds. The exceptions were
555 isolates *A. halophilicus* EXF-10623 and *A. creber* EXF-15148, of which formation was boosted
556 by carmine lake (*A. halophilicus* EXF-10623 by 3 % and *A. creber* EXF-15148 by 7 %; RH of 74
557 %), and isolates *C. halotolerans* EXF-15333 and *A. creber* EXF-15148, which were boosted by
558 the pigment lead white (*C. halotolerans* EXF-15333 by 10.2 % and *A. creber* EXF-15148 by 6.8
559 %; RH of 74 %).

560 Studies focusing on the identification of protein binders within painted model samples using the
561 enzyme-linked immunosorbent assay (ELISA) have shown that paints consisting of cochineal
562 lakes (carmine lakes), lead white, natural chalk, bone black, raw sienna or Verdigris contain
563 binding proteins (ovalbumin or casein) which are almost fully degraded [79,80], sometimes to the

564 extent that even antibodies, which are specific for these binding proteins, could not result in a
565 positive ELISA reaction. This high level of protein degradation was not detected for other kinds
566 of pigments. Therefore, in the case of lead white, important fungal proteins could undergo
567 enhanced degradation (preventing fungal development) due to the heavy metals within this paint.
568 As a matter of fact, interaction of lead (Pb^{+2}) with proteins (protein misfolding disorders and
569 aggregation of nascent proteins) represents a fundamental mechanism by which Pb^{+2} exerts
570 toxicity [81,82].

571 Carminic acid within the pigment carmine lake can even enhance fungal biomass growth and even
572 though its nutrimental role is unclear it may be involved in fungal melanin synthesis as it directly
573 elevates the activity of the enzyme laccase (catalyses the formation of melanin by oxidizing L-
574 DOPA) [83–85]. Moreover, Fernandes et al. [86] have shown that the inhibition of the melanin
575 synthesis in the fungus *Alternaria infectoria* results in the accumulation of the pigment carmine
576 red rather than in an albino phenotype. Therefore, it is most probable that aluminium and calcium
577 salts, which are added to complex the carminic acid into a natural carmine pigment [87,88] are
578 responsible for protein degradation. Aluminium reacts via the hexa-aqua trivalent species $Al^{3+}_{(aq)}$,
579 [89] and ligates to oxygen-based functional groups, principally through aluminium substitution for
580 competitive cations such as Ca^{2+} and Mg^{2+} , disrupting the functionality of various proteins [90–
581 92]. For example, even at low concentration (10 μM), $Al^{3+}_{(aq)}$ stimulates the level of ubiquitin
582 within murine neuroblastoma (NBP2) cell cultures [93]. The ubiquitin proteasome pathway is
583 highly conserved within eukaryotes (from fungi to mammals) and its function is to tag proteins for
584 their final destruction mediating the levels of cell cycle regulators and transcription factors
585 involved in morphogenesis [94]. The link between aluminium and the ubiquitin-mediated protein
586 degradation has also been observed in plants [95,96] and although similar responses in fungi have

587 not yet been investigated, various fungal species show intolerance of aluminium at concentrations
588 of as low as 500 ppm [97,98].

589
590 On the other hand, Prussian blue, an inorganic microcrystalline iron(III) hexacyanoferrate(II), may
591 represent a rich and easy source of iron which is essential for many biochemical processes within
592 a fungal cell, such as the synthesis of deoxyribonucleotides, respiration, the tricarboxylic acid
593 cycle, and the synthesis of numerous small molecules such as amino acids, lipids and sterols [99].
594 Recently, Planý et al. [100] observed fungal-induced atmospheric iron corrosion within the Natural
595 History Museum in London. The mechanism they describe includes the establishment of a fungal
596 based biofilm, the production of a corrosive electrolyte within the biofilm, transport of ions and
597 biomineralisation of iron-rich minerals.

598
599 Our observations confirm that tolerance to paint is species or strain dependent. For example,
600 isolates EXF-14897 and ZIM-F42, both identified as *A. niger*, had remarkably different growth
601 responses. Isolate EXF-14897 grew on Prussian blue as well as on lead white paint, however, the
602 formation of ZIM-F42 on any of the paints was non-existent. In accordance, for strain dependent
603 tolerance to lead, Sayer et al. [101] observed that some strains of *A. niger* could produce lead
604 oxalate dihydrate via the pyromorphite transformation process, which is the first recorded biogenic
605 solubilised formation of lead.

606 Overall, our results show that even at RH level as low as 55 %, which some experts regard as the
607 border line for fungal growth in museum environments [18], certain xerophilic fungal species can
608 still contaminate a painted surface, especially if it is wood supported and if the pigment present is

609 iron based. Considering the whole, however, the comparison between standard microbiological
610 tests (for xerophilic trait) and our incubator based tests indicates that fungi with a standardly
611 proven xerophilic trait may still fail to develop on painted model samples subjected to a low RH.

612

613

614

615

616

617

618

619

620

621

622

623

624

625

626

627

628 **6. Conclusions**

629 In this study we have investigated the xerophilic trait of 11 fungal isolates which were mostly
630 obtained from cultural heritage institutions. These were inoculated onto painted model samples
631 and incubated in monoculture in specially designed incubators with RH levels of 55 %, 63 % or
632 74 %. The following conclusions can be drawn:

633
634 1. Six isolates (*E. album* EXF-10689, *Aureobasidium melanogenum* EXF-15047, *P.*
635 *crustosum* ZIM-F94, *Aspergillus destruens* EXF-7651, *A. halophilicus* EXF-10623 and
636 *Wallemia* sp. EXF-10201) grew exclusively on wood based control samples.

637 2. At RH of 55 %, 2 isolates exhibited a slight growth; at RH of 63 %, the growth of 10
638 isolates was moderate to strong; 4 of these showed an additional increase in growth at RH
639 of 74 % (all examined on Prussian blue painted wood).

640 3. In comparison to the control samples (only binder), Prussian blue pigment within the
641 painted model samples increased the growth of isolates *P. crustosum* ZIM-F94, *Aspergillus*
642 *destruens* EXF-7651, *A. halophilicus* EXF-10623, *Wallemia* sp. EXF-10201 and
643 *Aureobasidium pullulans* EXF-150. In contrast, pigments carmine lake and lead white
644 generally completely prevented fungal growth with some isolates being tolerant
645 exceptions.

646 4. Fungi with a standardly proven xerophilic trait may still fail to develop on painted model
647 samples subjected to a low RH at 23 °C for a period of 120 days.

648

649

650

651 **Acknowledgements**

652

653 The authors would like to thank the European Commission for funding the InnoRenew CoE
654 project under the Horizon2020 Widespread-Teaming program (grant agreement ID: 739574;
655 start-up project 6.1. Advanced materials for cultural heritage storage); and the Slovenian
656 Research Agency for the next grants: J7-1815 and BI-RS/20-21-013. We are grateful to prof.
657 Bernarda Kosel for her grammatical corrections and to prof. dr. Polona Zalar (Department of
658 Biology, Biotechnical Faculty, University of Ljubljana) and prof. dr. Neža Čadež (Department of
659 Food Science and Technology, Biotechnical Faculty, University of Ljubljana) for their donations
660 of fungal isolates.

661

662

663

664

665

666

667

668

669

670

671

672

673

674

675

676

677

678

679 **Figure captions**

680

681 Figure 1: Incubator with paint samples on glass (A) and wood (B).

682

683 Figure 2: Fluorescent microscopic photographs used for determination of mould
684 surface coverage (on the photographs, *A. destruens* after 68 days of incubation on wood painted
685 with Prussian blue at an RH level of 63 % is presented). A: original photograph; B: black and white
686 8 bit photograph; C: boundary focus determination between the mould and the background; D:
687 binary format with black background and white mould; E: inverted image; and F: noise removal.

688 Figure 3: Percentage of growth of 11 fungal isolates on wooden and glass model samples painted
689 with egg temperas containing three different pigments (lead white, Prussian blue, carmine lake).
690 Incubation continued for 120 days at a specific RH (55 %, 63 % or 74 %) and percentage of fungal
691 expansion over the surface was determined under the fluorescent microscope.

692 Figure 4: Fungal growth on wood based model samples under optical and fluorescent microscopy.
693 Initial (A; 28 days on incubation) and developed (B; 68 days on incubation) growth of *A. destruens*
694 EXF-7651 on wood with carmine lake egg tempera at RH of 74 % and analysed under optical
695 microscopy. Overgrowth of EXF-7651 (C) and *P. crustosum* ZIM-F94 (D) (68 days on incubation
696 at RH of 74 %; carmine lake egg tempera on wood) under fluorescence microscopy after
697 Calcofluor White staining.

698 Figure 5: Percentage of growth of 11 fungal isolates on glass (A) and wooden (B) control samples
699 containing only a layer of the whole egg binder. Incubation at RH of 74 % was terminated after 68

700 days and the percentage of fungal formation on the surface was determined under the fluorescent
701 microscope.

702

703 **Table captions**

704

705 Table 1: Eleven fungal strains isolated mostly from cultural heritage institutions' interiors.

706 Table 2: Xerophilic and hydrolytic potential of examined fungal isolates.

707

708

709 **References**

710

- 711 [1] F. Poyatos, F. Morales, A.W. Nicholson, A. Giordano, Physiology of biodeterioration on
712 canvas paintings, *J. Cell. Physiol.* 233 (2018) 2741–2751.
713 <https://doi.org/10.1002/jcp.26088>.
- 714 [2] M. del M. López-Miras, I. Martín-Sánchez, Á. Yebra-Rodríguez, J. Romero-Noguera, F.
715 Bolívar-Galiano, J. Ettenauer, K. Sterflinger, G. Piñar, Contribution of the Microbial
716 Communities Detected on an Oil Painting on Canvas to Its Biodeterioration, *PLoS One.* 8
717 (2013) e80198. <https://doi.org/10.1371/journal.pone.0080198>.
- 718 [3] L.R. Gobakken, M. Westin, Surface mould growth on five modified wood substrates
719 coated with three different coating systems when exposed outdoors, *Int. Biodeterior.*
720 *Biodegrad.* 62 (2008) 397–402. <https://doi.org/10.1016/j.ibiod.2008.03.004>.
- 721 [4] P. Guiamet, S. Borrego, P. Lavin, I. Perdomo, S.G. de Saravia, Biofouling and
722 biodeterioration in materials stored at the Historical Archive of the Museum of La Plata,
723 Argentine and at the National Archive of the Republic of Cuba, *Colloids Surfaces B*
724 *Biointerfaces.* 85 (2011) 229–234. <https://doi.org/10.1016/j.colsurfb.2011.02.031>.
- 725 [5] E.L. Krüger, W. Diniz, Relationship between indoor thermal comfort conditions and the
726 Time Weighted Preservation Index (TWPI) in three Brazilian archives, *Appl. Energy.* 88
727 (2011) 712–723. <https://doi.org/10.1016/j.apenergy.2010.09.011>.
- 728 [6] K. Sterflinger, F. Pinzari, The revenge of time: Fungal deterioration of cultural heritage
729 with particular reference to books, paper and parchment, *Environ. Microbiol.* 14 (2012)
730 559–566. <https://doi.org/10.1111/j.1462-2920.2011.02584.x>.
- 731 [7] J. Kosel, P. Ropret, Overview of fungal isolates on heritage collections of photographic
732 materials and their biological potency, *J. Cult. Herit.* 48 (2021) 277–291.
733 <https://doi.org/10.1016/j.culher.2021.01.004>.
- 734 [8] D. Grabek-Lejko, A. Tekiela, I. Kasprzyk, Risk of biodeterioration of cultural heritage
735 objects, stored in the historical and modern repositories in the Regional Museum in
736 Rzeszow (Poland). A case study, *Int. Biodeterior. Biodegrad.* 123 (2017) 46–55.
737 <https://doi.org/10.1016/j.ibiod.2017.05.028>.
- 738 [9] S. Capodicasa, S. Fedi, A.M. Porcelli, D. Zannoni, The microbial community dwelling on
739 a biodeteriorated 16th century painting, *Int. Biodeterior. Biodegrad.* 64 (2010) 727–733.
740 <https://doi.org/10.1016/j.ibiod.2010.08.006>.
- 741 [10] K. Sterflinger, G. Piñar, Microbial deterioration of cultural heritage and works of art -
742 Tilting at windmills?, *Appl. Microbiol. Biotechnol.* 97 (2013) 9637–9646.
743 <https://doi.org/10.1007/s00253-013-5283-1>.
- 744 [11] R.A. Samson, J. Houbraken, R.C. Summerbell, B. Flannigan, J.D. Miller, Common and
745 important species of fungi and actinomycetes in indoor environments. *Microorganisms in*
746 *home and indoor work environments: diversity, health impacts, investigation and control,*
747 *CRC Press. Boca Rat.* (2002) 247–266.

- 748 [12] T. Meklin, T. Reponen, C. McKinstry, S.H. Cho, S.A. Grinshpun, A. Nevalainen, A.
749 Veepsäläinen, R.A. Haugland, G. LeMasters, S.J. Vesper, Comparison of mold
750 concentrations quantified by MSQPCR in indoor and outdoor air sampled simultaneously,
751 *Sci. Total Environ.* 382 (2007) 130–134. <https://doi.org/10.1016/j.scitotenv.2007.03.031>.
- 752 [13] T. Meklin, R.A. Haugland, T. Reponen, M. Varma, Z. Lummus, D. Bernstein, L.J.
753 Wymer, S.J. Vesper, Quantitative PCR analysis of house dust can reveal abnormal mold
754 conditions, *J. Environ. Monit.* 6 (2004) 615–620. <https://doi.org/10.1039/b400250d>.
- 755 [14] G.S. De Hoog, J. Guarro, M.J. Figueras, J. Gené, Atlas of clinical fungi. 3rd CD-ROM ed,
756 Utrecht, Netherlands CBS-KNAW Fungal Biodivers. Cent. (2009).
- 757 [15] K. Abe, Assessment of home environments with a fungal index using hydrophilic and
758 xerophilic fungi as biologic sensors, *Indoor Air.* 22 (2012) 173–185.
759 <https://doi.org/10.1111/j.1600-0668.2011.00752.x>.
- 760 [16] Y. Saijo, A. Kanazawa, A. Araki, K. Morimoto, K. Nakayama, T. Takigawa, M. Tanaka,
761 E. Shibata, T. Yoshimura, H. Chikara, R. Kishi, Relationships between mite allergen
762 levels, mold concentrations, and sick building syndrome symptoms in newly built
763 dwellings in Japan, *Indoor Air.* 21 (2011) 253–263. <https://doi.org/10.1111/j.1600-0668.2010.00698.x>.
- 765 [17] A.I. Terr, Sick Building Syndrome: is mould the cause?, *Med. Mycol.* 47 (2009) S217–
766 S222. <https://doi.org/10.1080/13693780802510216>.
- 767 [18] K. Sterflinger, Fungi: Their role in deterioration of cultural heritage, *Fungal Biol. Rev.* 24
768 (2010) 47–55. <https://doi.org/10.1016/j.fbr.2010.03.003>.
- 769 [19] P. Manimohan, S. Mannethody, *Zygosporium gibbum*: a new and remarkable rust
770 hyperparasite, *Mycosphere.* 2 (2011) 219–222.
- 771 [20] A.A. Haleem Khan, S. Mohan Karuppayil, Fungal pollution of indoor environments and
772 its management, *Saudi J. Biol. Sci.* 19 (2012) 405–426.
773 <https://doi.org/10.1016/j.sjbs.2012.06.002>.
- 774 [21] K.F. Nielsen, Mycotoxin production by indoor molds, *Fungal Genet. Biol.* 39 (2003) 103–
775 117. [https://doi.org/10.1016/S1087-1845\(03\)00026-4](https://doi.org/10.1016/S1087-1845(03)00026-4).
- 776 [22] N. Deschuyffeleer, A. Vermeulen, J. Daelman, E. Castelein, M. Eeckhout, F. Devlieghere,
777 Modelling of the growth/no growth interface of *Wallemia sebi* and *Eurotium herbariorum*
778 as a function of pH, aw and ethanol concentration, *Int. J. Food Microbiol.* 192 (2015) 77–
779 85. <https://doi.org/10.1016/j.ijfoodmicro.2014.09.022>.
- 780 [23] J. Szostak-Kotowa, Biodeterioration of textiles, in: *Int. Biodeterior. Biodegrad.*, Elsevier,
781 2004: pp. 165–170. [https://doi.org/10.1016/S0964-8305\(03\)00090-8](https://doi.org/10.1016/S0964-8305(03)00090-8).
- 782 [24] B. Ankersmit, M.H.L. Stappers, Understanding the Indoor Climate, in: *Manag. Indoor*
783 *Clim. Risks Museums*, Springer International Publishing, 2017: pp. 141–187.
- 784 [25] M.S. Rakotonirainy, L.B. Vilmont, B. Lavédrine, A methodology for detecting the level of
785 fungal contamination in the French Film Archives vaults, *J. Cult. Herit.* 19 (2016) 454–
786 462. <https://doi.org/10.1016/j.culher.2015.12.007>.

- 787 [26] A.A. Sakr, M.F. Ali, M.F. Ghaly, M.E.S.F. Abdel-Haliem, Discoloration of ancient
788 Egyptian mural paintings by streptomycetes strains and methods of its removal, *Int. J.*
789 *Conserv. Sci.* 3 (2012) 249–258.
- 790 [27] N. Unković, M.L. Grbić, M. Stupar, Ž. Savković, A. Jelikić, D. Stanojević, J. Vukojević,
791 Fungal-Induced Deterioration of Mural Paintings: *In Situ* and Mock-Model Microscopy
792 Analyses, *Microsc. Microanal.* 22 (2016) 410–421.
793 <https://doi.org/10.1017/S1431927616000544>.
- 794 [28] N. Unković, M. Ljaljević Grbić, G. Subakov-Simić, M. Stupar, J. Vukojević, A. Jelikić,
795 D. Stanojević, Biodeteriogenic and toxigenic agents on 17th century mural paintings and
796 façade of the old church of the Holy Ascension (Veliki Krčimir, Serbia), *Indoor Built*
797 *Environ.* 25 (2016) 826–837. <https://doi.org/10.1177/1420326X15587178>.
- 798 [29] R.J. Koestler, *Art, biology, and conservation : biodeterioration of works of art*, Yale
799 University Press, 2004.
- 800 [30] N. Unković, I. Dimkić, M. Stupar, S. Stanković, J. Vukojević, M.L. Grbić, Biodegradative
801 potential of fungal isolates from sacral ambient: In vitro study as risk assessment
802 implication for the conservation of wall paintings, *PLoS One.* 13 (2018) 1–16.
803 <https://doi.org/10.1371/journal.pone.0190922>.
- 804 [31] N. Unković, S. Erić, K. Šarić, M. Stupar, Savković, S. Stanković, O. Stanojević, I.
805 Dimkić, J. Vukojević, M. Ljaljević Grbić, Biogenesis of secondary mycogenic minerals
806 related to wall paintings deterioration process, *Micron.* 100 (2017) 1–9.
807 <https://doi.org/10.1016/j.micron.2017.04.004>.
- 808 [32] C. Abrusci, D. Marquina, A. Santos, A. Del Amo, T. Corrales, F. Catalina, A
809 chemiluminescence study on degradation of gelatine. Biodegradation by bacteria and
810 fungi isolated from cinematographic films, 2007.
811 <https://doi.org/10.1016/j.jphotochem.2006.06.003>.
- 812 [33] C. Abrusci, A. Martín-González, A. Del Amo, T. Corrales, F. Catalina, Biodegradation of
813 type-B gelatine by bacteria isolated from cinematographic films. A viscometric study,
814 *Polym. Degrad. Stab.* 86 (2004) 283–291.
815 <https://doi.org/10.1016/j.polymdegradstab.2004.04.024>.
- 816 [34] C. Abrusci, D. Marquina, A. Santos, A. Del Amo, F. Catalina, Bacteria present in
817 cinematographic films stored in spanish archives . Biodegradation of photographic
818 gelatine, *Biodegradation.* 661 (2006).
- 819 [35] M. Bučková, A. Puškárová, M.C. Sclocchi, M. Bicchieri, P. Colaizzi, F. Pinzari, D.
820 Pangallo, Co-occurrence of bacteria and fungi and spatial partitioning during photographic
821 materials biodeterioration, *Polym. Degrad. Stab.* 108 (2014) 1–11.
822 <https://doi.org/10.1016/j.polymdegradstab.2014.05.025>.
- 823 [36] M. Kwiatkowska, R. Ważny, K. Turnau, A. Wójcik, Fungi as deterioration agents of
824 historic glass plate negatives of Brandys family collection, *Int. Biodeterior. Biodegrad.*
825 115 (2016) 133–140. <https://doi.org/10.1016/j.ibiod.2016.08.002>.
- 826 [37] M.J.L. Lourenço, J.P. Sampaio, Microbial deterioration of gelatin emulsion photographs:

- 827 Differences of susceptibility between black and white and colour materials, *Int.*
828 *Biodeterior. Biodegrad.* 63 (2009) 496–502. <https://doi.org/10.1016/j.ibiod.2008.10.011>.
- 829 [38] O.E. Craig, M.J. Collins, The removal of protein from mineral surfaces: Implications for
830 residue analysis of archaeological materials, *J. Archaeol. Sci.* 29 (2002) 1077–1082.
831 <https://doi.org/10.1006/jasc.2001.0757>.
- 832 [39] G. Bingley, J. Verran, Counts of fungal spores released during inspection of mouldy
833 cinematographic film and determination of the gelatinolytic activity of predominant
834 isolates, *Int. Biodeterior. Biodegrad.* 84 (2013) 381–387.
835 <https://doi.org/10.1016/j.ibiod.2012.04.006>.
- 836 [40] A. Tulsi Ram, Archival preservation of photographic films - A perspective, *Polym.*
837 *Degrad. Stab.* 29 (1990) 3–29.
- 838 [41] J.D. Gu, D.T. Eberiel, S.P. McCarthy, R.A. Gross, Cellulose acetate biodegradability upon
839 exposure to simulated aerobic composting and anaerobic bioreactor environments, *J.*
840 *Environ. Polym. Degrad.* 1 (1993) 143–153. <https://doi.org/10.1007/BF01418207>.
- 841 [42] H.M. Szczepanowska, D. Jha, T.G. Mathia, Morphology and characterization of
842 Dematiaceous fungi on a cellulose paper substrate using synchrotron X-ray
843 microtomography, scanning electron microscopy and confocal laser scanning microscopy
844 in the context of cultural heritage, *J. Anal. At. Spectrom.* 30 (2015) 651–657.
845 <https://doi.org/10.1039/c4ja00337c>.
- 846 [43] N.S. Allen, M. Edge, J.H. Appleyard, T.S. Jewitt, C. V. Horie, D. Francis, Degradation of
847 historic cellulose triacetate cinematographic film: The vinegar syndrome, *Polym. Degrad.*
848 *Stab.* 19 (1987) 379–387. [https://doi.org/10.1016/0141-3910\(87\)90038-3](https://doi.org/10.1016/0141-3910(87)90038-3).
- 849 [44] A. Borrego, S., Molina, A., Santana, Fungi in Archive Repositories Environments and the
850 Deterioration of the Graphics Documents, *EC Microbiol.* 11 (2017) 205–226.
- 851 [45] S. Borrego, A. Molina, A. Santana, Mold on Stored Photographs and Maps : A Case
852 Study, *Top. Photogr. Preserv.* 16 (2015) 109–120.
- 853 [46] K.P. Koutsoumanis, J.N. Sofos, Effect of inoculum size on the combined temperature, pH
854 and a w limits for growth of *Listeria monocytogenes*, *Int. J. Food Microbiol.* 104 (2005)
855 83–91. <https://doi.org/10.1016/j.ijfoodmicro.2005.01.010>.
- 856 [47] Ž. Jurjević, A. Kubátová, M. Kolařík, V. Hubka, Taxonomy of *Aspergillus* section
857 *Petersonii* sect. nov. encompassing indoor and soil-borne species with predominant
858 tropical distribution, *Plant Syst. Evol.* 301 (2015) 2441–2462.
859 <https://doi.org/10.1007/s00606-015-1248-4>.
- 860 [48] F. Sklenář, Jurjević, P. Zalar, J.C. Frisvad, C.M. Visagie, M. Kolařík, J. Houbraeken, A.J.
861 Chen, N. Yilmaz, K.A. Seifert, M. Coton, F. Déniel, N. Gunde-Cimerman, R.A. Samson,
862 S.W. Peterson, V. Hubka, Phylogeny of xerophilic aspergilli (subgenus *Aspergillus*) and
863 taxonomic revision of section *Restricti*, *Stud. Mycol.* 88 (2017) 161–236.
864 <https://doi.org/10.1016/j.simyco.2017.09.002>.
- 865 [49] S.W. Peterson, Z. Jurjević, *Talaromyces columbinus* sp. nov., and genealogical
866 concordance analysis in *Talaromyces* clade 2a., *PLoS One.* 8 (2013) 78084.

- 867 <https://doi.org/10.1371/journal.pone.0078084>.
- 868 [50] P. Raspor, F. Cus, K.P. Jemec, T. Zagorc, N. Cadez, J. Nemanic, Yeast population
869 dynamics in spontaneous and inoculated alcoholic fermentations of Zametovka must,
870 Food Technol. Biotechnol. 40 (2002) 95–102.
- 871 [51] C. Gostinčar, R.A. Ohm, T. Kogej, S. Sonjak, M. Turk, J. Zajc, P. Zalar, M. Grube, H.
872 Sun, J. Han, A. Sharma, J. Chiniquy, C.Y. Ngan, A. Lipzen, K. Barry, I. V. Grigoriev, N.
873 Gunde-Cimerman, Genome sequencing of four *Aureobasidium pullulans* varieties:
874 Biotechnological potential, stress tolerance, and description of new species, BMC
875 Genomics. 15 (2014) 1–29. <https://doi.org/10.1186/1471-2164-15-549>.
- 876 [52] P.E.L. Van Tieghem, *Aspergillus niger*, Annu. Sci. Natl. Bot. 5 (1867) 240.
- 877 [53] J.I. Pitt, A.D. Hocking, Fungi and food spoilage, 519th ed., Springer US, New York, 2009.
878 https://doi.org/10.1007/978-0-387-92207-2_1.
- 879 [54] A. Puškárová, M. Bučková, B. Habalová, L. Kraková, A. Maková, D. Pangallo, Microbial
880 communities affecting albumen photography heritage: A methodological survey, Sci. Rep.
881 6 (2016) 1–14. <https://doi.org/10.1038/srep20810>.
- 882 [55] P. Dietemann, N. Wibke, O. Eva, R. Pogendorf, E. Reinkowski-Häfner, S. Heike,
883 Tempera painting between 1800 and 1950 Experiments and innovations from the
884 Nazarene movement to abstract art, Archetype Books, 2018.
- 885 [56] D.D. Perkins, Preservation of *Neurospora* stock cultures with anhydrous silica gel, Can. J.
886 Microbiol. 8 (1962) 591–594.
- 887 [57] D. Cadena-Herrera, J.E. Esparza-De Lara, N.D. Ramírez-Ibañez, C.A. López-Morales,
888 N.O. Pérez, L.F. Flores-Ortiz, E. Medina-Rivero, Validation of three viable-cell counting
889 methods: Manual, semi-automated, and automated, Biotechnol. Reports. 7 (2015) 9–16.
890 <https://doi.org/10.1016/j.btre.2015.04.004>.
- 891 [58] M.D. Abràmoff, P.J. Magalhães, S.J. Ram, Image processing with ImageJ, Biophotonics
892 Int. 11 (2004) 36–42.
- 893 [59] G.W. Zack, W.E. Rogers, S.A. Latt, Automatic measurement of sister chromatid exchange
894 frequency, J. Histochem. Cytochem. 25 (1977) 741–753.
895 <https://doi.org/10.1177/25.7.70454>.
- 896 [60] D.H. Wang, T.F. Ni, X.M. Ju, G.Y. Wei, Sodium chloride improves pullulan production
897 by *Aureobasidium pullulans* but reduces the molecular weight of pullulan, Appl.
898 Microbiol. Biotechnol. 102 (2018) 8921–8930. [https://doi.org/10.1007/s00253-018-9292-](https://doi.org/10.1007/s00253-018-9292-y)
899 [y](https://doi.org/10.1007/s00253-018-9292-y).
- 900 [61] H. Jiang, N.N. Liu, G.L. Liu, Z. Chi, J.M. Wang, L.L. Zhang, Z.M. Chi, Melanin
901 production by a yeast strain XJ5-1 of *Aureobasidium melanogenum* isolated from the
902 Taklimakan desert and its role in the yeast survival in stress environments, Extremophiles.
903 20 (2016) 567–577. <https://doi.org/10.1007/s00792-016-0843-9>.
- 904 [62] W. Wang, S. Li, Z. Chen, Z. Li, Y. Liao, J. Chen, Secondary Metabolites Produced by the
905 Deep-Sea-Derived Fungus *Engyodontium album*, Chem. Nat. Compd. 53 (2017) 224–226.

- 906 <https://doi.org/10.1007/s10600-017-1957-8>.
- 907 [63] A. Jaouani, M. Neifar, V. Prigione, A. Ayari, I. Sbissi, S. Ben Amor, S. Ben Tekaya, G.C.
908 Varese, A. Cherif, M. Gtari, Diversity and enzymatic profiling of halotolerant
909 micromycetes from Sebkha El Melah, a Saharan salt flat in Southern Tunisia, *Biomed*
910 *Res. Int.* (2014). <https://doi.org/10.1155/2014/439197>.
- 911 [64] A. Landa, R.R. Vázquez, T.G.R. Carillo, Mycoremediation of an Agricultural Salty Soil
912 Contaminated With Endosulfan by *Penicillium Crustosum*, (2020).
- 913 [65] J.H. Skalski, J.J. Limon, P. Sharma, M.D. Gargus, C. Nguyen, J. Tang, A.L. Coelho, C.M.
914 Hogaboam, T.R. Crother, D.M. Underhill, Expansion of commensal fungus *Wallemia*
915 *mellicola* in the gastrointestinal mycobiota enhances the severity of allergic airway disease
916 in mice, *PLOS Pathog.* 14 (2018) e1007260. <https://doi.org/10.1371/journal.ppat.1007260>.
- 917 [66] W. van Hartingsveldt, I.E. Mattern, C.M.J. van Zeijl, P.H. Pouwels, C.A.M.J.J. van den
918 Hondel, Development of a homologous transformation system for *Aspergillus niger* based
919 on the *pyrG* gene, *MGG Mol. Gen. Genet.* 206 (1987) 71–75.
920 <https://doi.org/10.1007/BF00326538>.
- 921 [67] B.C.T. Schirmer, J. Wiik-Nielsen, I. Skaar, The mycobiota of the production
922 environments of traditional Norwegian salted and dried mutton (pinnekjøtt), *Int. J. Food*
923 *Microbiol.* 276 (2018) 39–45. <https://doi.org/10.1016/j.ijfoodmicro.2018.04.007>.
- 924 [68] E. V. Smolyanyuk, E.N. Bilanenko, Communities of halotolerant micromycetes from the
925 areas of natural salinity, *Microbiology.* 80 (2011) 877–883.
926 <https://doi.org/10.1134/S002626171106021X>.
- 927 [69] S. Chellappan, C. Jasmin, S.M. Basheer, A. Kishore, K.K. Elyas, S.G. Bhat, M.
928 Chandrasekaran, Characterization of an extracellular alkaline serine protease from marine
929 *Engyodontium album* BTMFS10, *J. Ind. Microbiol. Biotechnol.* 38 (2011) 743–752.
930 <https://doi.org/10.1007/s10295-010-0914-3>.
- 931 [70] M.S. Park, S. Lee, S.Y. Oh, G.Y. Cho, Y.W. Lim, Diversity and enzyme activity of
932 *Penicillium* species associated with macroalgae in Jeju Island, *J. Microbiol.* 54 (2016)
933 646–654. <https://doi.org/10.1007/s12275-016-6324-0>.
- 934 [71] R. Chamekh, F. Deniel, C. Donot, J.L. Jany, P. Nodet, L. Belabid, Isolation, Identification
935 and Enzymatic Activity of Halotolerant and Halophilic Fungi from the Great Sebkha of
936 Oran in Northwestern of Algeria, *Mycobiology.* 47 (2019) 230–241.
937 <https://doi.org/10.1080/12298093.2019.1623979>.
- 938 [72] T. Vitisant, W. Leelaruij, W. Chulalaksananukul, A high-activity lipolytic yeast isolated
939 from Sichang Island , *Maejo Int. J. Sci. Technol.* 7 (2013) 96–105.
- 940 [73] C. Alapont, P. V. Martínez-Culebras, M.C. López-Mendoza, Determination of lipolytic
941 and proteolytic activities of mycoflora isolated from dry-cured teruel ham, *J. Food Sci.*
942 *Technol.* 52 (2015) 5250–5256. <https://doi.org/10.1007/s13197-014-1582-5>.
- 943 [74] N.D. Mahadik, U.S. Puntambekar, K.B. Bastawde, J.M. Khire, D. V. Gokhale, Production
944 of acidic lipase by *Aspergillus niger* in solid state fermentation, *Process Biochem.* 38
945 (2002) 715–721. [https://doi.org/10.1016/S0032-9592\(02\)00194-2](https://doi.org/10.1016/S0032-9592(02)00194-2).

- 946 [75] T.J.K. Strang, 4. Dry, cool and contained, in: Stud. Pest Control Cult. Prop., University of
947 Gothenburg, Gothenburg, 2012: p. 115.
- 948 [76] O. Guillitte, Bioreceptivity: a new concept for building ecology studies, *Sci. Total*
949 *Environ.* 167 (1995) 215–220. [https://doi.org/10.1016/0048-9697\(95\)04582-L](https://doi.org/10.1016/0048-9697(95)04582-L).
- 950 [77] K.S. Modes, E.J. Santini, M.A. Vivian, Hygroscopicity of wood from *Eucalyptus grandis*
951 and *Pinus taeda* subjected to thermal treatment, *Cerne.* 19 (2013) 19–25.
952 <https://doi.org/10.1590/S0104-77602013000100003>.
- 953 [78] K. Sedlbauer, M. Krus, Schimmelpilz aus bauphysikalischer Sicht, Fraunhofer-Institut Fū
954 r Bauphysik, Holzkirchen. 45 (2003).
- 955 [79] F. Ren, N. Atlasevich, B. Baade, J. Loike, J. Arslanoglu, Influence of pigments and
956 protein aging on protein identification in historically representative casein-based paints
957 using enzyme-linked immunosorbent assay, *Anal. Bioanal. Chem.* 408 (2016) 203–215.
958 <https://doi.org/10.1007/s00216-015-9089-0>.
- 959 [80] T. Špec, S. Peljhan, J. Vidič, N.L. Krajnc, M. Fonović, Č. Tavzes, P. Ropret, CIM®
960 monolith chromatography-enhanced ELISA detection of proteins in artists' paints:
961 Ovalbumin as a case study, *Microchem. J.* 127 (2016) 102–112.
962 <https://doi.org/10.1016/j.microc.2016.02.004>.
- 963 [81] P.L. Goering, Lead-protein interactions as a basis for lead toxicity, *Neurotoxicology.* 14
964 (1993) 45–60.
- 965 [82] M.J. Tamás, S.K. Sharma, S. Ibstedt, T. Jacobson, P. Christen, Heavy metals and
966 metalloids as a cause for protein misfolding and aggregation, *Biomolecules.* 4 (2014) 252–
967 267. <https://doi.org/10.3390/biom4010252>.
- 968 [83] C. Hernández, A.M. Farnet Da Silva, F. Ziarelli, I. Perraud-Gaime, B. Gutiérrez-Rivera,
969 J.A. García-Pérez, E. Alarcón, Laccase induction by synthetic dyes in *Pycnoporus*
970 *sanguineus* and their possible use for sugar cane bagasse delignification, *Appl. Microbiol.*
971 *Biotechnol.* 101 (2017) 1189–1201. <https://doi.org/10.1007/s00253-016-7890-0>.
- 972 [84] R.J.N. Frandsen, P. Khorsand-Jamal, K.T. Kongstad, M. Nafisi, R.M. Kannangara, D.
973 Staerk, F.T. Okkels, K. Binderup, B. Madsen, B.L. Møller, U. Thrane, U.H. Mortensen,
974 Heterologous production of the widely used natural food colorant carminic acid in
975 *Aspergillus nidulans*, *Sci. Rep.* 8 (2018) 1–10. <https://doi.org/10.1038/s41598-018-30816-9>.
- 976
- 977 [85] D. Lee, E.H. Jang, M. Lee, S.W. Kim, Y. Lee, K.T. Lee, Y.S. Bahna, Unraveling melanin
978 biosynthesis and signaling networks in *Cryptococcus neoformans*, *MBio.* 10 (2019).
979 <https://doi.org/10.1128/mBio.02267-19>.
- 980 [86] C. Fernandes, R. Prados-Rosales, B.M.A. Silva, A. Nakouzi-Naranjo, M. Zuzarte, S.
981 Chatterjee, R.E. Stark, A. Casadevall, T. Gonçalves, Activation of melanin synthesis in
982 *Alternaria infectoria* by antifungal drugs, *Antimicrob. Agents Chemother.* 60 (2016)
983 1646–1655. <https://doi.org/10.1128/AAC.02190-15>.
- 984 [87] J. Kirby, M. Van Bommel, A. Verhecken, Natural colorants for dyeing and lake pigments:
985 practical recipes and their historical sources, Archetype Publications London, 2014.

- 986 [88] D. Cardon, *Natural dyes: Sources, tradition, technology and science*, (2007) 268.
- 987 [89] R.B. Martin, The chemistry of aluminum as related to biology and medicine, *Clin. Chem.*
988 32 (1986) 1797–1806. <https://doi.org/10.1093/clinchem/32.10.1797>.
- 989 [90] T.L. Macdonald, R. Bruce Martin, Aluminum ion in biological systems, *Trends Biochem.*
990 *Sci.* 13 (1988) 15–19. [https://doi.org/10.1016/0968-0004\(88\)90012-6](https://doi.org/10.1016/0968-0004(88)90012-6).
- 991 [91] C. Exley, J.D. Birchall, The cellular toxicity of aluminium, *J. Theor. Biol.* 159 (1992) 83–
992 98.
- 993 [92] T. Kiss, M. Hollósi, The Interaction of Aluminium with Peptides and Proteins, in: *Alum.*
994 *Alzheimer's Dis.*, Elsevier, 2001: pp. 361–392. [https://doi.org/10.1016/b978-044450811-](https://doi.org/10.1016/b978-044450811-9/50044-6)
995 [9/50044-6](https://doi.org/10.1016/b978-044450811-9/50044-6).
- 996 [93] A. Campbell, A. Kumar, F.G. La Rosa, K.N. Prasad, S.C. Bondy, Aluminum Increases
997 Levels of beta-Amyloid and Ubiquitin in Neuroblastoma But Not in Glioma Cells, *Proc.*
998 *Soc. Exp. Biol. Med.* 223 (2000) 397–402. [https://doi.org/10.1046/j.1525-](https://doi.org/10.1046/j.1525-1373.2000.22356.x)
999 [1373.2000.22356.x](https://doi.org/10.1046/j.1525-1373.2000.22356.x).
- 1000 [94] D. Kornitzer, The ubiquitin system and morphogenesis of fungal pathogens, *Isr. Med.*
1001 *Assoc. J.* 8 (2006) 243–245.
- 1002 [95] X. Qin, S. Huang, Y. Liu, M. Bian, W. Shi, Z. Zuo, Z. Yang, Overexpression of A RING
1003 finger ubiquitin ligase gene AtATRF1 enhances aluminium tolerance in *Arabidopsis*
1004 *thaliana*, *J. Plant Biol.* 60 (2017) 66–74. <https://doi.org/10.1007/s12374-016-0903-9>.
- 1005 [96] X. Zhang, N. Wang, P. Chen, M. Gao, J. Liu, Y. Wang, T. Zhao, Y. Li, J. Gai,
1006 Overexpression of a soybean ariadne-like ubiquitin ligase gene GmARI1 enhances
1007 aluminum tolerance in *Arabidopsis*, *PLoS One.* 9 (2014) 111120.
1008 <https://doi.org/10.1371/journal.pone.0111120>.
- 1009 [97] P. Illmer, R. Buttinger, Interactions between iron availability, aluminium toxicity and
1010 fungal siderophores, *BioMetals.* 19 (2006) 367–377. [https://doi.org/10.1007/s10534-005-](https://doi.org/10.1007/s10534-005-3496-1)
1011 [3496-1](https://doi.org/10.1007/s10534-005-3496-1).
- 1012 [98] G.W. Thompson, R.J. Medve, Effects of Aluminum and Manganese on the Growth of
1013 Ectomycorrhizal Fungi, *Appl. Environ. Microbiol.* 48 (1984) 556–560.
1014 <https://doi.org/10.1128/aem.48.3.556-560.1984>.
- 1015 [99] C.C. Philpott, Iron uptake in fungi: A system for every source, *Biochim. Biophys. Acta -*
1016 *Mol. Cell Res.* 1763 (2006) 636–645. <https://doi.org/10.1016/j.bbamcr.2006.05.008>.
- 1017 [100] M. Planý, F. Pinzari, K. Šoltys, L. Kraková, L. Cornish, D. Pangallo, A.D. Jungblut, B.
1018 Little, Fungal-induced atmospheric iron corrosion in an indoor environment, *Int.*
1019 *Biodeterior. Biodegrad.* 159 (2021) 105204. <https://doi.org/10.1016/j.ibiod.2021.105204>.
- 1020 [101] J.A. Sayer, J.D. Cotter-Howells, C. Watson, S. Millier, G.M. Gadd, Lead mineral
1021 transformation by fungi, *Curr. Biol.* 9 (1999) 691–694. [https://doi.org/10.1016/S0960-](https://doi.org/10.1016/S0960-9822(99)80309-1)
1022 [9822\(99\)80309-1](https://doi.org/10.1016/S0960-9822(99)80309-1).

1023